Tutor

Dr. Vicente Marchán Sancho
Departament de Química Inorgànica i Orgànica, Secció de Química Orgànica

Grau de Química

Treball Final de Grau

Synthesis and characterization of new coumarin-based COUPY fluorophores

Síntesi i caracterització de nous fluoròfors COUPY basats en cumarina

Joan Forcadell Ferré

June 2021

Universitat de Barcelona

B:KC Barcelona Knowledge Campus
Campus d'Excel·lència Internacional

Aquesta obra esta subjecta a la llicència de:
Reconeixement–NoComercial-SenseObraDerivada

http://creativecommons.org/licenses/by-nc-nd/3.0/es/

Intentarem posar llum a la foscor.

Carles Porta

En primer lloc, voldria agrair al meu tutor, el Dr. Vicente Marchán Sancho, per la seva ajuda en la planificació i organització del treball i la seva dedicació durant tota la recerca.

També vull agrair a les meves companyes i companys de la planta de Química Orgànica que amb els seus coneixements i recolzament m'han guiat a través de cada una de les etapes d'aquest projecte per obtenir els resultats que buscava. En especial, dono les gracies a l'Anna Rovira, no hagués pogut arribar a aquests resultats sense la seva incondicional ajuda.

Per acabar, un agraïment no menys sincer a la meva família i amics per el suport moral i emocional proporcionat dia a dia.

Moltes gràcies a tots.

REPORT

CONTENTS

1. SUMMARY

The availability of fluorophores based on small organic molecules operating in the optical window of biological tissues enables the precise interrogation of biochemical and biological systems. Among coumarin-based fluorophores, COUPY dyes are particularly interesting for developing novel cellular and molecular imaging tools due to their promising physicochemical and photophysical properties, such as excellent cell permeability, large Stokes' shifts, high photostability and absorption and emission in the far-red/near-infrared (NIR) region, the latter being important to minimize photodamage to living cells.

In this work, we have focused on the synthesis and characterization of four new COUPY dyes with the aim of improving their photophysical properties as well as to allow the labelling of targeting ligands by incorporating suitable functional groups within the coumarin scaffold.

Keywords: coumarin, organic fluorophore, organic synthesis, bioimaging.

2. RESUM

L'ús de fluoròfors basats en petites molècules orgàniques que operen a la finestra òptica dels teixits biològics permet la interrogació precisa de sistemes bioquímics i biològics. Entre els fluoròfors basats en cumarina, els derivats COUPY són particularment interessants per desenvolupar noves eines d'imatge cel·lular i molecular gràcies a les seves prometedores propietats fisicoquímiques i fotofísiques, com ara una excel·lent permeabilitat cel·lular, grans desplaçaments de Stokes, una elevada fotoestabilitat i absorció i emissió en la regió entre el vermell llunyà i l'infraroig proper (NIR), sent aquesta darrera característica molt important per minimitzar el dany a les cèl·lules vives.

En aquest treball, ens hem centrat en la síntesi i caracterització de quatre nous fluoròfors COUPY amb l'objectiu de millorar les seves propietats fotofísiques, així com permetre el marcatge de lligands dirigits mitjançant la incorporació de grups funcionals adequats dins de l'estructura de la cumarina.

Paraules clau: cumarina, fluoròfor, síntesi orgànica, bioimatge .

3. INTRODUCTION

3.1. FLUOROPHORES BASED ON SMALL ORGANIC MOLECULES

The process of fluorescence is exemplified by the Jablonski diagram (Figure 1).[1] Absorption of photons (light energy) by molecules promotes them from a singlet electronic ground state (S_0) to a singlet excited state (S_1, S_2, etc.). In this process, an electron is promoted first to a higher energy orbital, which relaxes rapidly to the first singlet excited state (S_1). Fluorescence occurs when this excited state relaxes to ground state with photon emission. Alternatively, the excited state can relax through nonradiative (NR) processes, including molecular collision, bond rotation or vibration, and photoinduced electron transfer (PeT). When photon emission from the triplet state (T_1) occurs, the process is named phosphorescence. In general, the maximum emission wavelength is higher due to energy lost by solvent reorganization or other processes. The difference between maximum absorption wavelength (λ_{max}) and the maximum emission wavelength (λ_{em}) is termed the "Stokes' shift".

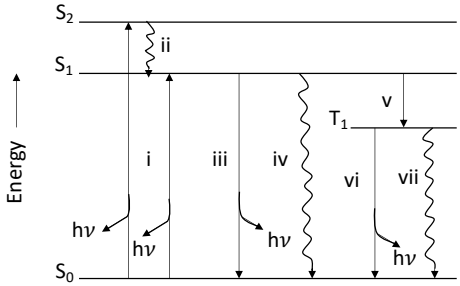

Figure 1. Jablonski diagram (i) absorption of a photon gives an excited state, (ii) internal conversion to S_1, (iii) fluorescence emission, (iv) nonradiative decay, (v) intersystem crossing to T_1, (vi) phosphorescence emission, (vii) nonradiative decay.

Nowadays, fluorophores based on small organic molecules represent an indispensable tool in chemical biology applications. Fluorescence provides a mechanism for achieving contrast in biological imaging techniques as well as for *in vivo* detection and/or quantification of biologically

relevant species.[2] Fluorophores are also used for labelling biomolecules such as peptides, proteins and oligonucleotides, enzyme substrates, environmental indicators, and cellular stains.[1]

An ideal organic fluorophore is one that maximizes signal and minimizes noise.[2] In general, the large collection of fluorescent probes is derived from a humble set of "core" scaffolds. Some examples of the most common fluorophores are shown in Figure 2: endogenous fluorophores like quinine (**1**), the boron dipyrromethene (BODIPY) dyes (**2**), fluoresceins (**3**), rhodamines (**4**), phenoxazines (**5**), cyanines (**6**) and coumarins (**7**).[3]

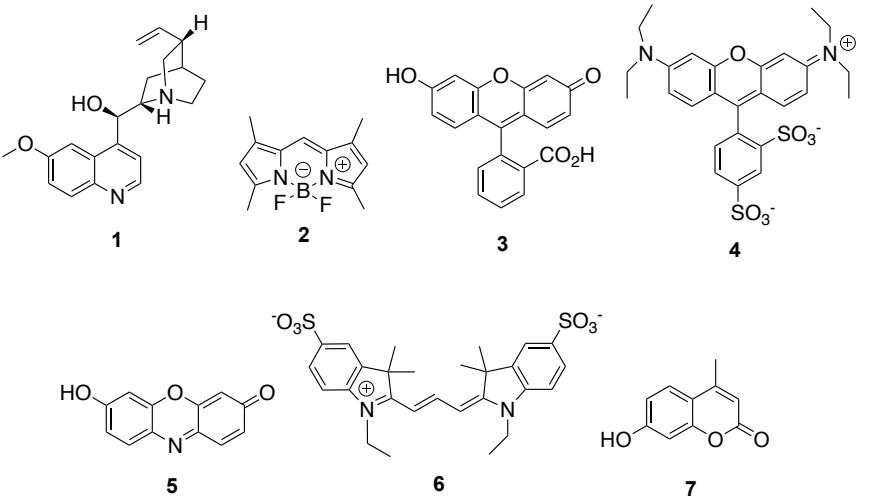

Figure 2. Structure of some typical organic fluorophores.

Among them, organic fluorophores with absorption and emission in the far-red/near-infrared (NIR) region of the electromagnetic spectrum (650-900 nm) are in great demand for biological applications. This radiation is especially useful due to several features such as the low tissue attenuation resulting in high penetration depth, minimum background autofluorescence and low light scattering, while minimizing photodamage to living cells compared to UV and blue light.[4], [5] Even so, most of the current far-red/NIR fluorescent dyes are far from being ideal due to their large molecular size and structural complexity. For this reason, great efforts are in progress to develop novel organic fluorophores operating in the optical window of biological tissues with optimal photophysical properties (absorption and emission maxima in the far red and NIR region, high fluorescence quantum yields and lifetimes, large Stokes' shifts and high photostability) and physicochemical properties (aqueous solubility and cell permeability).

3.2. COUMARINS

Coumarins are a well-known family of naturally-occurring molecules with a diverse range of pharmacological and biological activities owing to the privileged structure and physicochemical properties of the 2-benzopyrone moiety.[6] Since the discovery of Umbelliferone (7-hydroxycoumarin) at the end of the 19th century, coumarins have also been traditionally used as organic fluorophores due to their well-stablished photophysical properties and good cell membrane permeability.[7] The prototypical fluorescent coumarin is 4-methyl-7-hydroxy-coumarin (4-methylumbelliferone, 4-MU, **7**). Under basic conditions, the phenolate form of 4-MU (pK_a = 7.8) absorbs UV light (λ_{max} = 360 nm, $\varepsilon = 1.7 \times 10^4$ M^{-1} cm^{-1}) and emits blue light (λ_{em} = 450 nm, Φ = 0.63).[2]

Conventional coumarins such as 4-MU need UV excitation. However, as previously stated, UV and blue light difficult nearly all *in vivo* applications due to the inherent toxicity and poor penetration in biological tissues of this radiation. Since coumarins are amenable to smart structural modifications to easily tune their photophysical properties, great efforts have been dedicated in the last decades to red-shift absorption and emission of coumarins into the blue-green-red region of the visible spectrum by increasing the electronic delocalization along the π-conjugated system. In addition, these modifications can be done at the late synthetic stages, facilitating conjugation to a broad variety of targeting ligands including lipids, peptides, proteins, oligonucleotides, and antibodies.[8],[9]

The fluorescence emission of the classical coumarin scaffold can be shifted from blue to cyan via the insertion of electron-donating groups such as *N,N*-dialkylamino at position 7 of the coumarin skeleton (**8**, Figure 3) that partner with the electron-withdrawing lactone moiety to create a push-pull effect. Moreover, the incorporation of strong additional electron-withdrawing groups (EWGs) like CF_3, CN or carboxyl at positions 3 and/or 4 has been reported to also red-shift the emission of these fluorophores.[6],[7] More recently, some groups have demonstrated that absorption and emission of coumarin-based fluorophores can additionally be red-shifted through modification of the lactone function. For instance, the thiocoumarin (**9**) leads to blue absorption ($\lambda_{max} \sim$ 470 nm) and green light emission ($\lambda_{max} \sim$ 550) in the *7-N,N*-diethylamino series.[10] Another reported approach consists of the incorporation of a dicyanomethylene group which resulted in a red-shift effect in both absorption and emission (**10**).[11],[12] On 2017, our research group synthesized new coumarin derivatives in which one cyano group in dicyanocoumarin **10**

was replaced by a phenyl ring containing EWGs at *ortho* and *para* positions to increase the push-pull character of the chromophore (e.g., **11** in Figure 3). With this modification in hand new caging groups that could be photoremoved with visible light were also obtained and at the same time red-shifting absorption in the green-red region. Even so, a negative effect on the fluorescence emission of the compounds was found due to the incorporation of strong EWGs such as nitro.[9],[13]

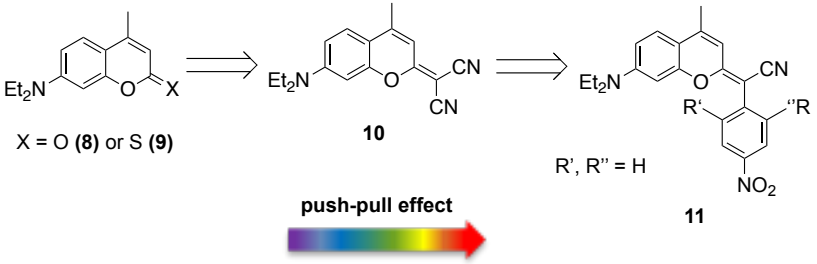

Figure 3. Rational design of new coumarin-based fluorophores.

3.3 COUMARIN-BASED FLUOROPHORES: COUPY DYES

As shown in Figure 4, our research group has recently developed a new family of coumarin-based fluorophores, nicknamed COUPY, in which one cyano group of dicyanocoumarin derivatives (**10**) was replaced by the electron-deficient pyridinium heterocycle (**12**) with the intention of further increasing the push-pull character of the coumarin chromophore whereas keeping a low molecular weight (MW 340-440). It is worth noting that COUPY's photophysical properties can be easily tuned by selecting the appropriate combination of the *N*-alkylating group at the pyridine moiety and electron-donating groups at position 7, which increase the intramolecular charge-transfer effect along the coumarin skeleton.

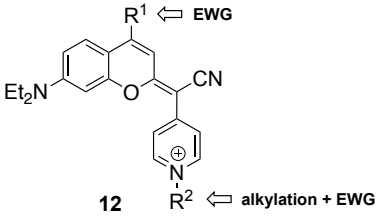

Figure 4. General structure of a COUPY dye.

Overall, COUPY dyes exhibit several appealing photophysical and physicochemical properties:[8]

i) far-red/NIR emission
ii) high photostability
iii) excellent brightness ($\varepsilon \times \Phi$)
iv) large Stokes' shifts
v) small, excellent cell membrane permeability
vi) accumulate selectively in nucleoli and/or mitochondria of HeLa cells
vii) smart synthesis

With the aim of improving the features of these compounds, our research group has reported several analogues of the original COUPY dyes (Figure 5). Azetidine introduction at position 7 (**13**), replacing *N,N*-diethyl- or *N,N*-dimethylamino groups, resulted in high photostability and enlarged Stokes' shifts but the quantum yield value (Φ) were not significantly modified in aqueous media. In addition, high cell permeability was retained.[7] Replacement of the *para*-pyridine heterocycle by *ortho*-pyridine (**14**) or *ortho,ortho*-pyrimidine (**15**) blue-shifted absorption and emission. However, the insertion of *ortho,para*-pyrimidine (**16**) provided novel photostable fluorophores with suitable photophysical properties, including emission in the far-red to NIR region and large Stokes' shifts. In addition, the compounds exhibited excellent cell membrane permeability in living cells and a higher selectivity for mitochondria than the parent compounds.[11] Finally, the transformation of COUPY fluorophores into novel class of visible-light-cleavable photolabile protecting groups (PPGs) (**17**) has been recently reported. COUPY-based PPGs overcome some of the limitations of classical caging groups owing to their increased push-pull character, which allows to perform uncaging with the biologically-compatible red light. [14]

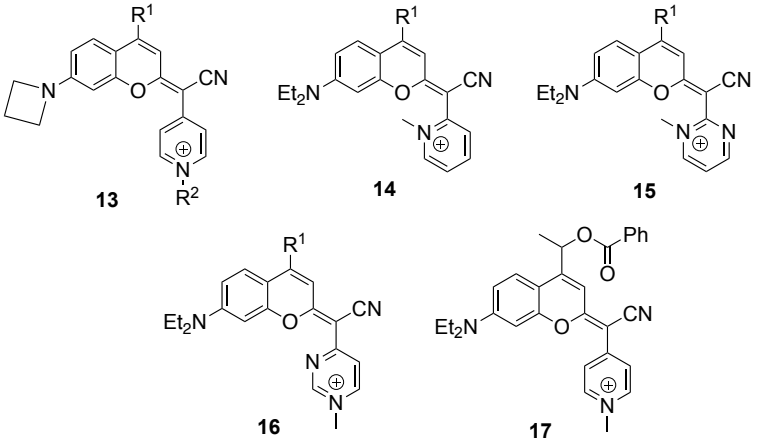

Figure 5. Examples of novel COUPY dyes and PPGs developed in our group.

With the aim of studying how the photophysical and physicochemical properties of the original COUPY dyes (e.g. **18**) are modified by cyclization around the *N,N*-dialkylamino group at 7-posicion, coumarin **19** has been recently synthesized in our research group (Figure 6) and found than an additional red-shift in the absorption maximum was achieved by this structural modification.[15] Taking into account all the antecedents, herein we focused on the synthesis and characterization of a new COUPY dye (**20**) with the aim of comparing its photophysical properties with those of the two parent compounds (**18** and **19**), specially to investigate if the incorporation of the methyl groups would enhance the push-pull effect and red-shift the absorption and emission maxima. In addition, in order to investigate the potential applications of this new COUPY dye in cellular imaging studies, we have also synthesized three derivatives incorporating ester (**21**), carboxyl (**22**) and Boc-protected amino groups (**23**) to allow labelling of targeting ligands.

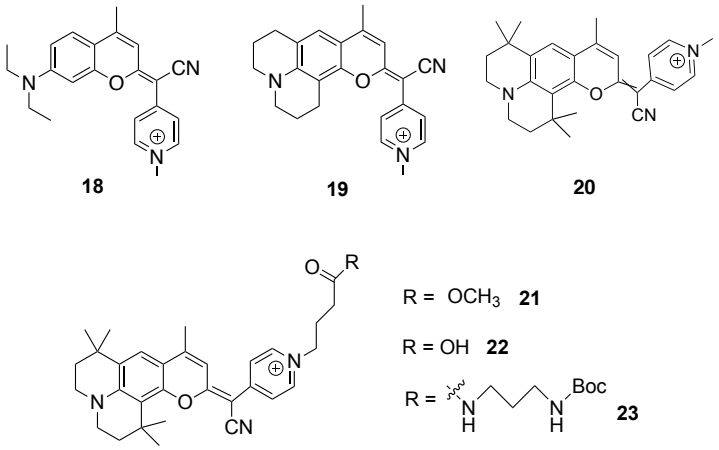

Figure 6. Structure of previously reported COUPY dyes (**18-19**) and of the new fluorophores synthesized in this work (**20-23**).

4. OBJECTIVES

In this work we have focused on the synthesis and characterization of four new COUPY dyes (**20-23**) to be used in bioimaging applications.

The specific objectives of this work were:

1) Synthesis and characterization of a thiocoumarin precursor (**24**).
2) Synthesis and characterization of a COUPY scaffold precursor (**25**).
3) Synthesis and characterization of COUPY dyes **20-23**.
4) Characterization of the compounds by 2D NOESY NMR experiments.
5) Confocal microscopy studies with COUPY dye **20** in living HeLa cells.

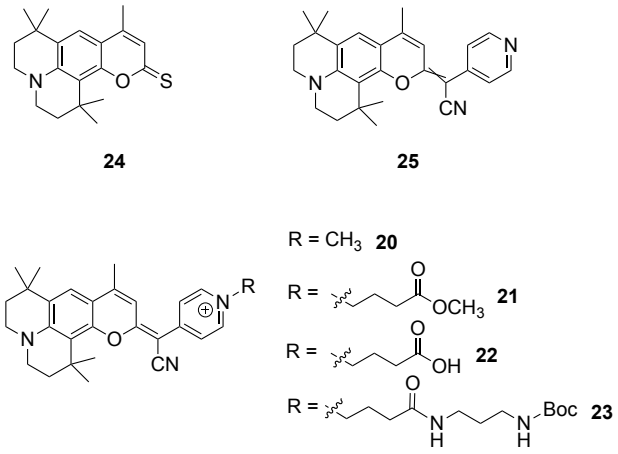

Figure 7. Structure of compounds synthesized in this work.

5. RESULTS AND DISCUSSION

The retrosynthetic analysis for the preparation of COUPY dyes **20-23** is shown in Scheme 1. First, the thiocoumarin derivative (**24**) will be obtained through thionation of the carbonyl group of the lactone function of commercially available coumarin (**26**) with Lawesson's reagent.[16] Then, condensation of the thiocarbonyl group of coumarin **24** with 4-pyridylacetonitrile will provide the key COUPY scaffold **25**. The synthesis of COUPY dye **20** was planned through with *N*-methylation of pyridine moiety of compound **25** with methyl triflate.[7]

On the other hand, *N*-alkylation of compound **25** with methyl 4-bromobutyrate will conduce to compound **21**. The acid hydrolysis of the ester function of **21** will afford coumarin **22**, in which a *N*-Boc-1,3-propanediamine linker will be attached via an amide bond to obtain the final product **23**.

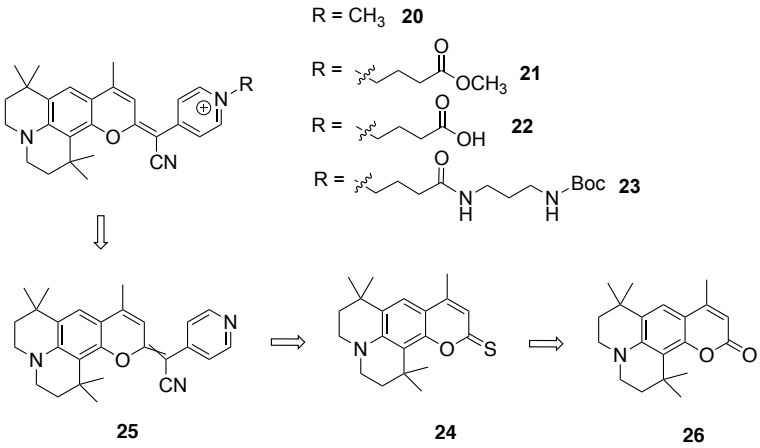

Scheme 1. Retrosynthetic analysis for the preparation of COUPY dyes **20-23**.

5.1. SYNTHESIS OF COUMARIN 20

The synthesis route followed for the preparation of compound **20** is shown in Scheme 2.

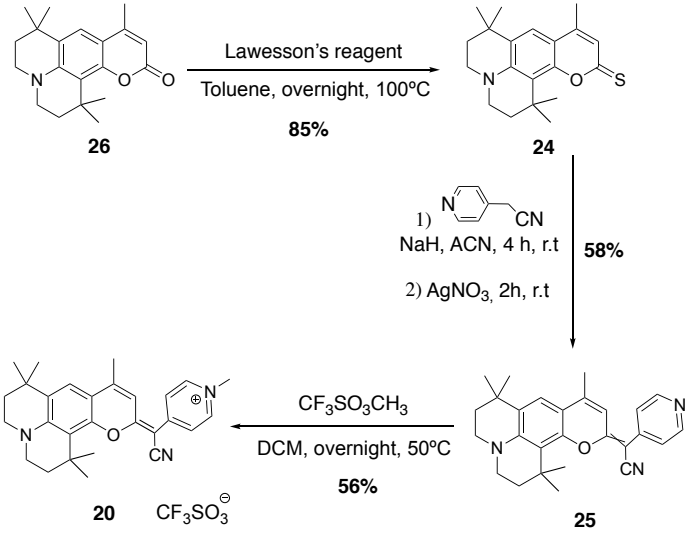

Scheme 2. Synthetic route followed for the preparation of **20**.

5.1.1. Synthesis of thiocoumarin 24

Starting with the commercially available coumarin **26**, reaction with Lawesson's reagent overnight at 100ºC conduced to the thiocoumarin **24**, which was purified by silica column chromatography (85 % yield) and characterized by ^{1}H and ^{13}C NMR and high-resolution mass spectrometry.

Lawesson's reagent has a four-membered ring of alternating phosphorus and sulphur atoms. Upon heating, the central four-membered ring is opened to form two more reactive dithiophosphine ylides, which react with a carbonyl group to generate a thiaoxaphosphetane intermediate. Then, the formation of a stable P=O bond forces cycloreversion step (Scheme 3).

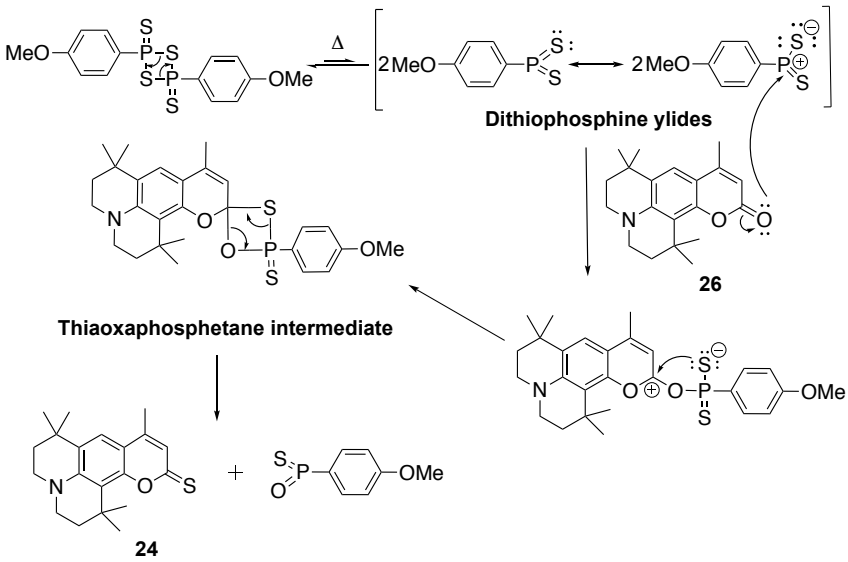

Scheme 3. Mechanism for the thionation of **26** by using Lawesson's reagent.

5.1.2. Synthesis of COUPY scaffold 25

The following step involved the condensation of 4-pyridylacetonitrile with the thiocarbonyl group of thiocoumarin **24** to give COUPY scaffold **25**. As shown in Scheme 4, 4-pyridylacetonitrile is deprotonated by using a strong base (NaH) giving a 4-pyridylacetonitrile carbanion, which is stabilized by resonance. This carbanion acts as a nucleophile and attacks thiocarbonyl group forming a tetrahedral intermediate. Treatment with $AgNO_3$ triggers the loss of the sulphur atom and the formation of compound **25**.

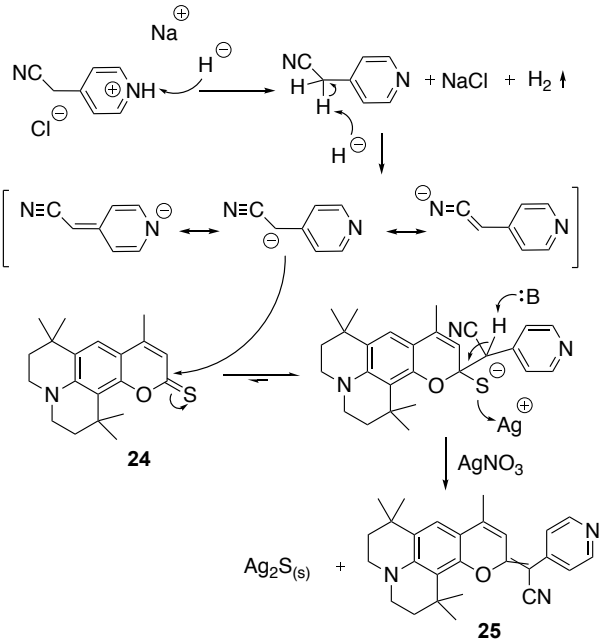

Scheme 4. Proposed mechanism for the condensation of 4-pyridylacetonitrile with **24**.

It is worth noting that the synthesis of coumarin scaffold **25** was optimized modifying the equivalents of NaH, maintaining all the other conditions. As shown in Table 1, the addition of 5 equivalents of NaH conduced to the best results. In addition, the use of potassium *tert*-butoxide as a base instead of NaH was also investigated. Unfortunately, the reaction of thiocoumarin **24** with this base did not afford the expected compound (**25**).

Table 1. Optimization of the synthesis of **25**.

Attempt	Amount of 24 [mg]	Base	Equivalents of Base	Yield [%][a]
1	150	NaH	8	38
2	816	NaH	20	*b*
3	844	NaH	40	*b*
4	500	NaH	20	*b*
5	500	NaH	5	58
6	3000	NaH	5	45

([a]) Isolated yield.
([b]) Not purified. Only traces of **25** were identified in the crude by HPLC-MS.

Compound **25** was isolated by silica column chromatography (45-58 % yield depending on the reaction scale) and fully characterized by ^{1}H and ^{13}C NMR, 2D NOESY NMR, and high-resolution mass spectrometry. The purity of the compound was assessed by HPLC-MS analysis revealing a single peak (Appendix 1).

Interestingly, the ^{1}H-NMR spectrum (Figure 8) of COUPY scaffold **25** showed the presence of two sets of proton signals in $CDCl_3$ in an ~65:35 ratio and the same duplicity was found in the ^{13}C NMR spectra.

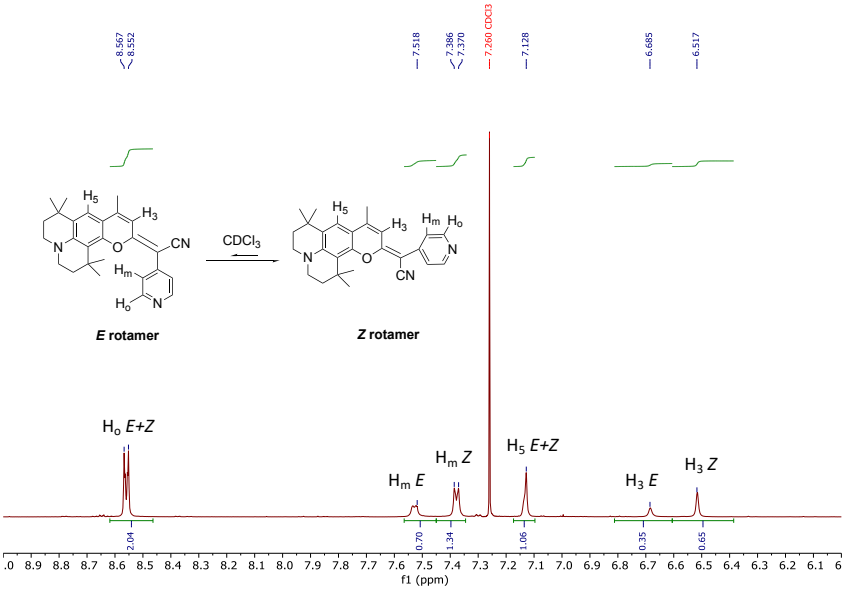

Figure 8. Aromatic region of the ^{1}H NMR spectrum of COUPY scaffold **25**.

Full assignment of the ^{1}H NMR spectrum by using 2D NOESY NMR experiment confirmed the presence of two species in slow equilibrium in the solution in the chemical shift time scale. (Figure 9).

As shown in Figure 10, the presence of chemical exchange cross-peaks in the 2D NOESY spectrum accounts for the existence of *E* and *Z* interconverting rotamers around the exocyclic C=C bond (Figure 9).

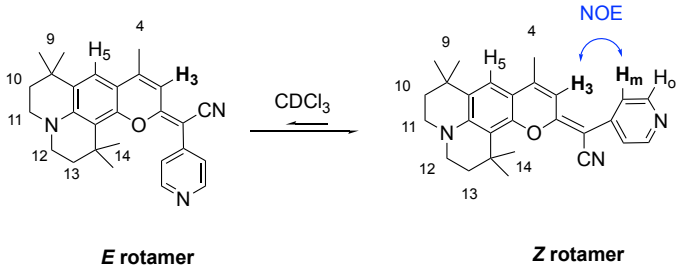

Figure 9. Structures of *E* and *Z* rotamers of COUPY scaffold **25** with one diagnostic NOE cross-peak indicated.

The existence of rotamers instead of diastereomers can be attributed to the strong push-pull character of the compound: the exocyclic C=C bond connecting C-2 of the coumarin moiety and C-4 of the pyridine cannot be considered a pure doble bond, but a double bond with partial single bond character due to the strong electronic delocalization along the π-conjugated system.

The presence of diagnostic NOE cross-peaks between the proton at position 3 of the coumarin in the major rotamer and the meta protons of the pyridine enabled us to conclude that the *Z* rotamer was the major one (therefore the one usually drawn in this work). This fact can be explained to the steric effect caused by the two methyl groups (14) of the cyclic amine at position 7, which destabilizes the rotamer *E*. Interestingly, a different behaviour was found for previous synthetized COUPY scaffold analogues in our research group, where rotamer *E* has always been observed as the major one.[9]

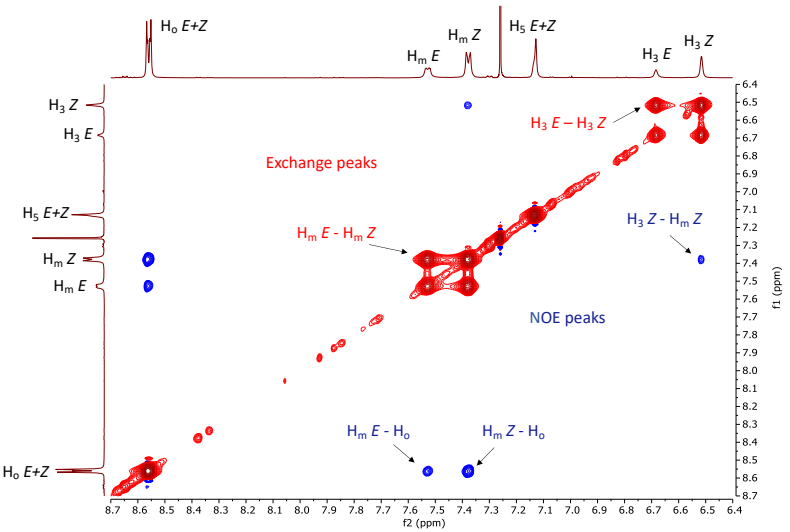

Figure 10. Aromatic region of the 2D NOESY spectrum of COUPY scaffold **25** in $CDCl_3$ showing exchange cross-peaks (red) between rotamer resonances and NOE cross-peaks (blue).

5.1.2. Synthesis of COUPY dye 20

The pyridine moiety of coumarin scaffold **25** was alkylated with methyl triflate in DCM overnight at 50ºC to generate the *N*-methylpyridinium-coumarin **20** (Scheme 5), which was isolated by silica column chromatography (56 % yield).

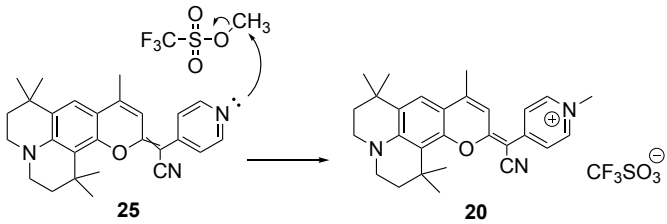

Scheme 5. Mechanism for the alkylation of **25** with methyl triflate.

Full characterization of compound **20** was carried out by ^{1}H and ^{13}C NMR, 2D NOESY NMR and HR-ESI MS and the purity of the compound was assessed by HPLC-MS analysis revealing a single peak (Appendix 1). In this case, the ^{1}H-NMR spectrum of compound **20** (Annex 2) showed only one set of proton signals. The lack of exchange cross-peaks and the presence of diagnostic NOE cross-peaks in the 2D NOESY NMR spectrum (Figure 11), such as the one between the H_3

proton of the coumarin and the meta protons of the pyridine allowed us to conclude that the rotamer *Z* was the only species in solution. It is worth noting that for coumarin analogue **18**, previously synthetized by our group, 2D NOESY NMR experiments accounted that rotamer *E* was the only species in solution.

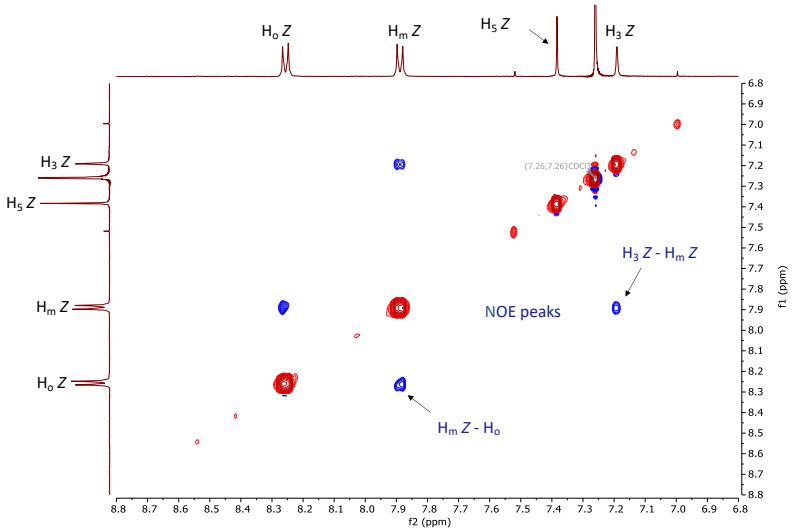

Figure 11. Aromatic region of the 2D NOESY spectrum of coumarin **20** in $CDCl_3$ showing NOE cross-peaks (blue).

5.2. SYNTHESIS OF COUMARINS 21, 22 AND 23

The synthesis route followed for the preparation of compounds **21-23** is shown in Scheme 6.

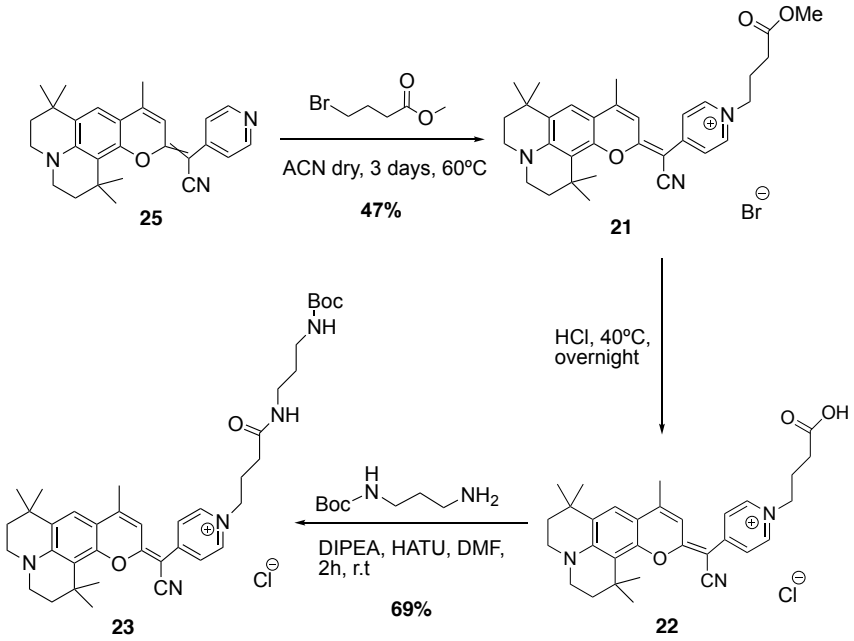

Scheme 6. Synthetic route followed for the preparation of coumarins **21-23**.

As shown in Schemes 6 and 7, *N*-alkylation of the pyridine moiety of COUPY scaffold **25** with methyl 4-bromobutyrate in ACN dry during 3 days at 60ºC conduced to the compound **21**.

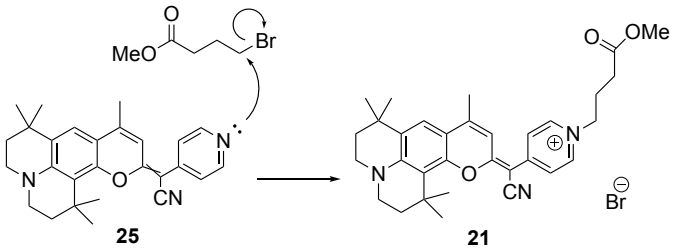

Scheme 7. Mechanism for the alkylation of **25** with methyl 4-bromobutyrate.

To our surprise, the HPLC-MS analysis of the reaction crude (Figure 12) revealed the presence of a side product with the same mass than the *N*-methylpyridinium coumarin (**20**).

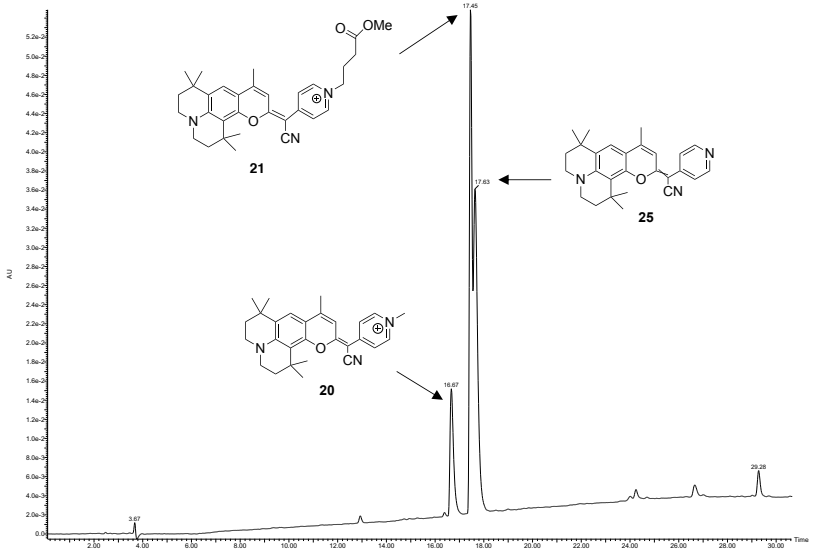

Figure 12. HPLC-MS chromatogram of the reaction crude for coumarin **21** after 72 h.

Both the desired compound **21** (47 % yield) and the side product were isolated by silica column chromatography. Subsequent characterization of the side product by ^{1}H NMR confirmed that compound **20** had been formed.

Taking into account the strange side reaction that occurred when using methyl 4-bromobutyrate, we decided to repeat it but with a different *N*-alkylating reagent (ethyl 4-bromobutyrate, 100 equivalents). After 1 day at 60 ºC, HPLC-MS analysis (Figure 13) showed the formation of the expected coumarin **27** without any other side product, which indicates that the formation of *N*-methylated coumarin is related with the use of methyl 4-bromobutyrate. Hence, ethyl 4-bromobutyrate would be a better option than methyl 4-bromobutyrate for the preparation of **22** and **23** from coumarin **27**.

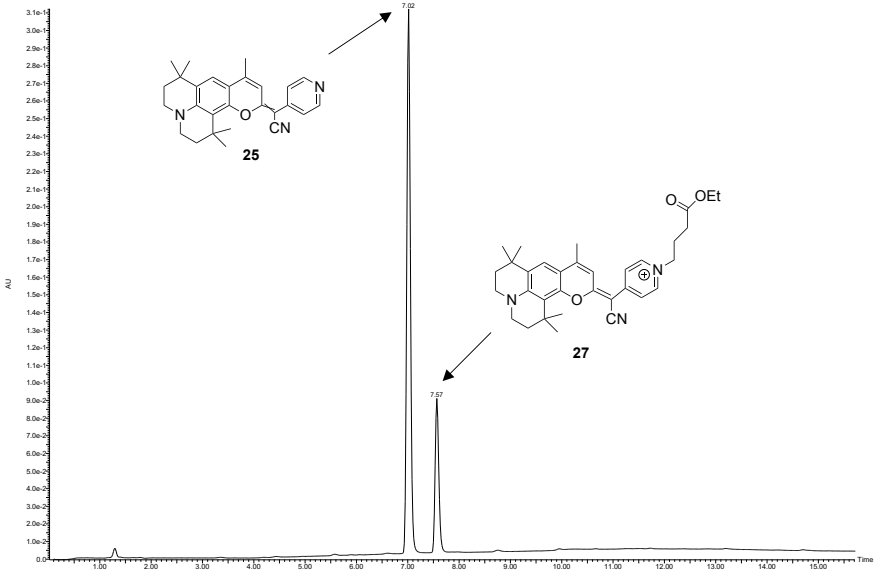

Figure 13. HPLC-MS chromatogram of the reaction crude for coumarin **27**.

Full characterization of compound **21** was carried out by ^{1}H and ^{13}C NMR, 2D NOESY NMR and HR-ESI-MS, and the purity was assessed by HPLC-MS analysis revealing a single peak (Annex 1).

As previously found for coumarin **20**, the ^{1}H-NMR spectrum of compound **21** (Annex 2) showed only one set of proton signals and again, ^{1}H-^{1}H NOESY experiments (Figure 14) confirmed that the rotamer *Z* was the only species in solution.

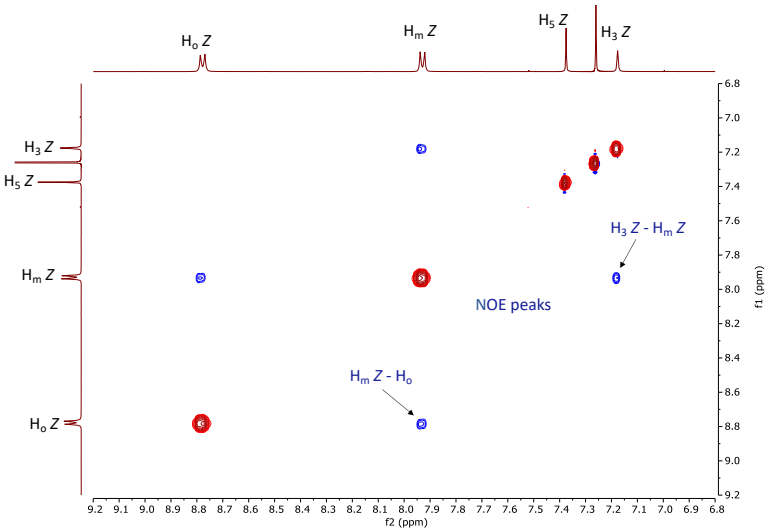

Figure 14. Aromatic region of the 2D NOESY spectrum of coumarin **21** in $CDCl_3$ showing NOE cross-peaks (blue).

Having at hand coumarin **21** we focused on the synthesis of compound **23** incorporating an amino group for labelling targeting ligands. Firstly, compound **21** was transformed into **22** bearing the carboxylic acid function by acidic hydrolysis with HCl at 40ºC overnight.[16] Unfortunately, this reaction afforded not only compound **22**, but also coumarin **26** and the pyridine-acetonitrile moiety due to the cleavage of the exocyclic bond under acidic conditions (Scheme 8). The reaction was repeated at 60ºC for 3,5 hours in order to reduce this side reaction. In this case, HPLC-MS analysis (Figure 15) showed the same side reaction but to a lesser extent and, consequently, we decided to use this crude without further purification in the next step.

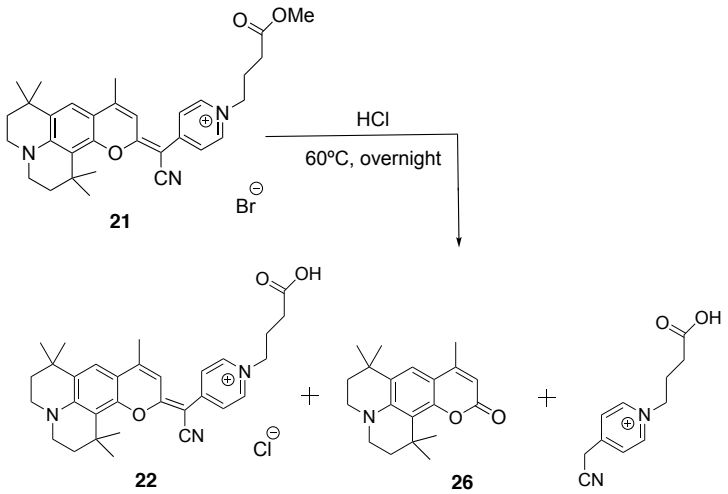

Scheme 8. Synthesis of compound **22** and side products generated.

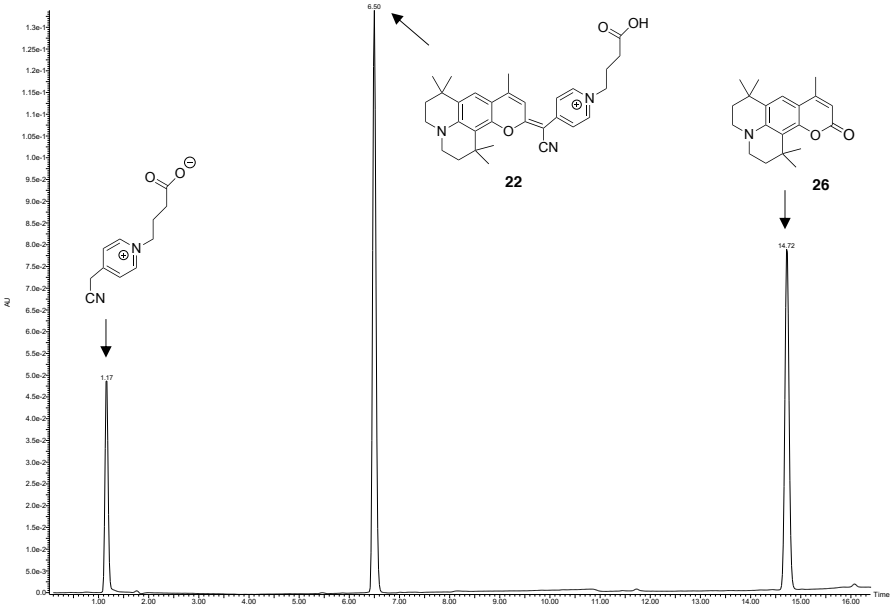

Figure 15. HPLC-MS analysis of the reaction crude for the synthesis of compound **22**.

Finally, N-Boc-1,3-propanediamine linker was attached to compound **22** by using HATU as a coupling reagent in the presence of DIPEA, to afford compound **23** (Scheme 9).

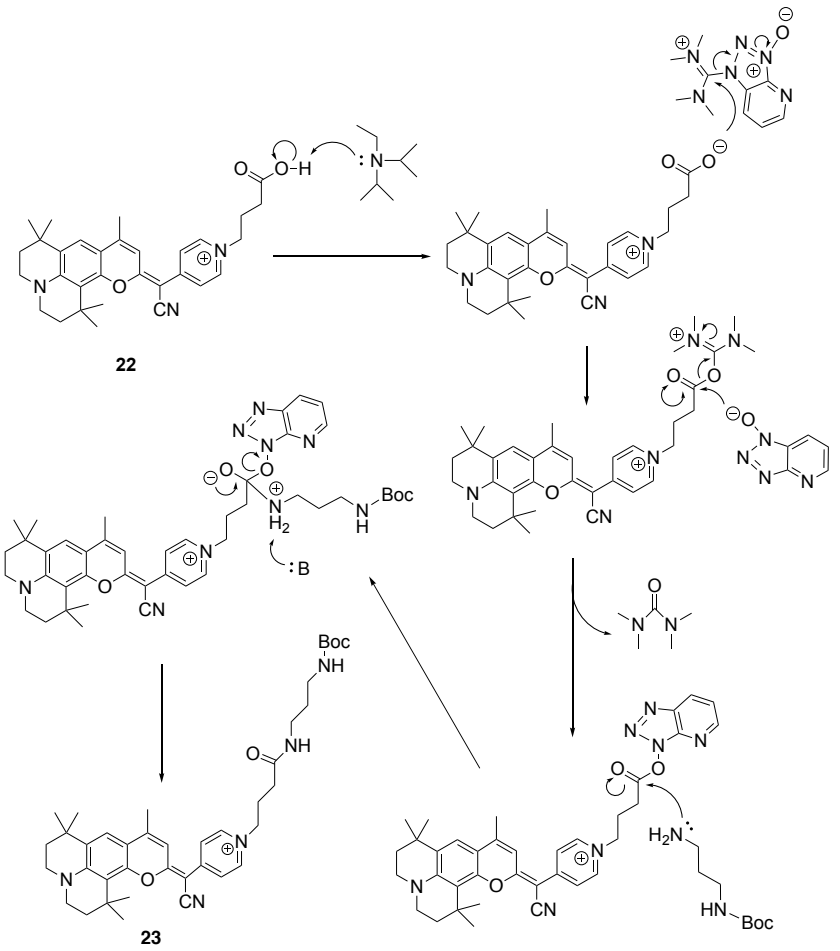

Scheme 9. Mechanism for the HATU-mediated formation of the amide bond in **23**.

The characterization of compound **23** was carried out by ^{1}H and ^{13}C NMR and HR-ESI-MS, the purity of the compound was assessed by HPLC-MS analysis revealing a single peak (Annex 1).

5.3. FLUORESCENCE IMAGING OF COUPY DYES IN LIVING CELLS

Due to the excellent photophysical properties of the fluorescent dyes based on COUPY scaffolds, our research group has investigated their potential applications in bioimaging. As an example, the cellular uptake of coumarin **18** (see structure in Figure 6) was studied in living HeLa cells by confocal microscopy by irradiation with a yellow light laser (λ_{ex} = 561 nm). Fluorescence after 20 min of incubation was clearly observed in mitochondria and intracellular vesicles and also, although less intensely, in the nucleoli.[9] The *N*-methylpyridinium group is a typical moiety that, due to his structure, makes these compounds to accumulate in the mitochondria. As shown in Figure 19, the same pattern of staining was recently observed for coumarin **19** (Figure 6) when irradiating with a yellow light laser (λ_{ex} = 561 nm) and with a red one (λ_{ex} = 633 nm).

On the basis of all these precedents, we investigated the cellular uptake of coumarin **20** in HeLa cells. Very interestingly, no significant fluorescence was detected in nucleoli, which suggests a higher preference of coumarin **20** for mitochondria compared with the parent coumarins **18** and **19** (Figure 16). Overall, these results provide new insights into the design and optimization of mitochondria-targeted fluorescent probes based on small organic molecules, since higher selectivity for this organelle can be achieved through the incorporation of methyl groups at the cyclic amine at position 7, which would difficult the insertion of the molecule in RNA in nucleoli.

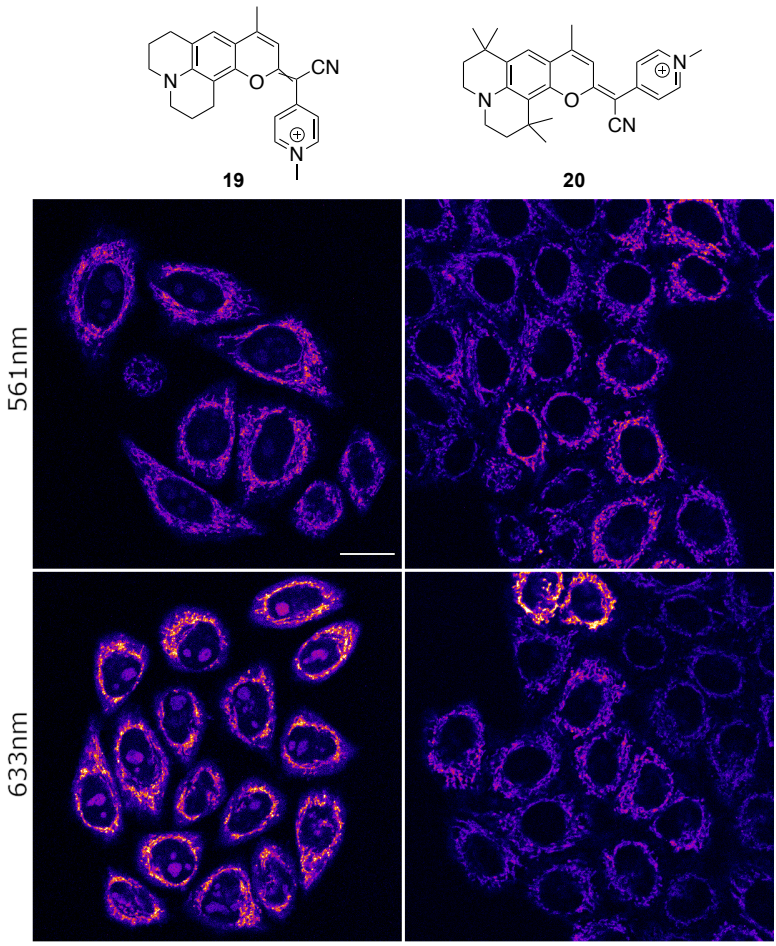

Figure 16. Comparison of the cellular uptake of coumarins **19** and **20** in living HeLa cells by confocal microscopy.

6. CONCLUSIONS

A new thiocoumarrin derivative (**24**) has been satisfactorily synthesized from commercially available coumarin **26** and characterized by spectroscopic techniques. The COUPY scaffold **25** was prepared with moderate yield by condensation of this thiocoumarin precursor with 4-pyridilacetonitrile. Coumarin **25** was fully characterized by ^{1}H and ^{13}C NMR, HPLC-MS and HRMS. In addition, 2D NOESY NMR experiments allowed us to demonstrate the existence of rotamers in solution in an ~65:35 ratio (*Z* and *E*, respectively) caused by the rotation around the exocyclic double bond, which cannot be considered a pure doble bond due to the strong π-delocalization. Subsequent *N*-allkylation of the pyridine moiety allowed the easy and efficient synthesis of coumarins **20** and **21**. Moreover, coumarin **23** has been prepared from coumarin **21** in two steps with the aim of labelling targeting ligands in the future. Finally, the cellular uptake of coumarin **20** in living HeLa cells was investigated by confocal microscopy revealing a higher preference for mitochondria compared with previously reported coumarins.

Overall, in this research work we have developed new COUPY fluorophores with potential applications for cell imaging.

7. EXPERIMENTAL SECTION

7.1. MATERIALS AND METHODS

7.1.1. Reagents and solvents

All reagents were supplied by Sigma Aldrich, Alfa Aesar, Fluorochem or Acros. The solvents and its quality and supplier are indicated in the following table:

Table 2.

Entry	Solvent	Quality	Suplier
1	Acetonitrile[(a)]	HPLC quality	Scharlau
2	CH_2Cl_2	HPLC quality	Fisher
3	CH_2Cl_2	Synthesis quality	SDS
4	DMF[(b)]	Synthesis quality	SDS
5	EtOH absolute	Synthesis quality	Panreac
6	Hexane	Synthesis quality	SDS
7	H_2O	Deionized	-
8	MeOH	Synthesis quality	Scharlau
9	Toluene	Synthesis quality	Scharlau

(a) ACN was dried by standing over 4Å molecular sieves.
(b) DMF was dried by standing over 4Å molecular sieves and bubbled with nitrogen to remove volatile amines.

7.1.2. Nuclear magnetic resonance spectroscopy (NMR)

All NMR spectra were recorded at 25ºC on Varian or Bruker 400MHz instruments, using $CDCl_3$ containing 0.03% (v/v) of TMS. Coupling constants (*J*) are given in Hz and the following abbreviations were used to indicate multiplicities: s, singlet; d, doublet; dd, doublet of doublets; t, triplet; q, quartet; qt, quintuplet; m, multiplet.

7.1.3. Chromatographic techniques

7.1.3.1. High-performance liquid chromatography (HPLC)

Reversed-phase HPLC analyses were carried out on a Waters instrument equipped with a diode array detector. The detection was carried out within the following range: 200-800 nm.

A Jupiter 4u Proteo column (Phenomenex, 250 x4.6 mm, 4 μm, 90 Å) was used at a constant flow (1 mL/min) using gradients of the following solvents: A (Formic acid 0.1% in H_2O), B (Formic acid 0.1% in ACN).

7.1.3.2. Thin layer chromatography (TLC)

TLC analyses were performed on aluminium plates coated with 0.2 μm, thick layer of silica gel (60F, 245nm, Merck). TLC was visualized directly under an UV lamp (245 nm and 365 nm).

7.1.3.3. Column Chromatography

Flash column chromatography was carried out with silica gel Chromatogel 60 Å (35-75 μm) from SDS.

7.1.4. Mass spectrometry

7.1.4.1. Electrospay ionization mass spectrometry (ESI-MS)

Electrospray ionization mass spectrometry analyses were carried out on a HPLC waters 2695 equipped with a Micromass ZQ quadrupole analyser and UV-Vis detector.

7.1.4.2. High resolution electrospray ionization mass spectrometry (HR ESI-MS)

High resolution electrospray ionization mass spectrometry analyses were carried out on a LC/MS-TOF instrument.

7.2. SYNTHESIS OF COUMARIN 24

Lawesson's reagent (7.79 g, 19.27 mmol) was added to a solution of coumarin **26** (10 g, 32.11 mmol) in toluene (250 mL). The resulting solution was stirred under reflux at 100ºC overnight and protected from light. The mixture was allowed to cool to room temperature and the solvent was removed under reduced pressure. The crude product was purified by column chromatography (silica gel, 0-100% DCM in hexane) to give 8.94 g (85% yield) of an orange solid.

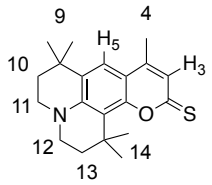

24

Orange solid.
^{1}H NMR ($CDCl_3$, 400 MHz) δ (ppm): 7.27 (s, 1H, H_5), 6.90 (s, 1H, H_3), 3.37 – 3.30 (m, 2H, H_{12}), 3.28 – 3.20 (m, 2H, H_{11}), 2.29 (s, 3H, H_4), 1.85 – 1.80 (m, 2H, H_{13}), 1.78 – 1.73 (m, 2H, H_{10}), 1.60 (s, 6H, H_{14}), 1.31 (s, 6H, H_9). ^{13}C NMR ($CDCl_3$, 101 MHz) δ (ppm): 195.7, 155.3, 146.6, 145.9, 129.7, 123.3, 119.6, 114.8, 111.7, 47.4, 47.0, 39.5, 35.7, 32.6, 32.4, 30.7, 29.2, 18.3. HRMS (ESI): *m/z* calcd. for $C_{20}H_{26}NOS$ $[M+H]^+$ 328.1730; found 328.1731
Rf (100% CH_2Cl_2) = 0.65

7.3. SYNTHESIS OF COUMARIN 25

Firstly, the reagents NaH (60% dispersion in mineral oil, 1.1 g, 45.8 mmol), 4-pyridylacetonitrile hydrochloride (2.12 g, 13.74 mmol) and the thiocoumarin **24** (3 g, 9.19 mmol) were dried overnight in a desiccator under vacuum. Secondly, the reagents were dissolved in anhydrous ACN (500 mL) under an Ar atmosphere in the dark and the mixture was stirred for 4 hours at room temperature. Next, $AgNO_3$ (3.42 g, 20.15 mmol) was added, and the reaction mixture was stirred for 2 hours under argon atmosphere and protected from light. Then, the solvent was removed under reduced pressure and the crude product was purified by column chromatography (silica gel, 0-2.5% MeOH in CH_2Cl_2) to give 1.70 g (45% yield) of a brown solid.

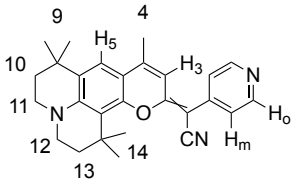

25

Brown solid.
^{1}H NMR ($CDCl_3$, 400 MHz) δ (ppm): Rotamer *E*: 8.59 – 8.47 (m, 2H, H_o), 7.60 – 7.46 (m, 2H, H_m), 7.13 (s, 1H, H_5), 6.68 (s, 1H, H_3), 3.37 – 3.25 (m, 2H, H_{12}), 3.24 – 3.13 (m, 2H, H_{11}), 2.31 (s, 3H, H_4), 1.85 – 1.80 (m, 2H, H_{13}), 1.79 – 1.71 (m, 2H, H_{10}), 1.66 (s, 6H, H_{14}), 1.30 (s, 6H, H_9). Rotamer *Z*: 8.59 – 8.47 (m, 2H, H_o), 7.46 – 7.33 (m, 2H, H_m), 7.13 (s, 1H, H_5), 6.52 (s, 1H, H_3), 3.37 – 3.25 (m, 2H, H_{12}), 3.24 – 3.13 (m, 2H, H_{11}), 2.26 (s, 3H, H_4), 1.85 – 1.80 (m, 2H, H_{13}), 1.79 – 1.71 (m, 2H, H_{10}), 1.66 (s, 6H, H_{14}), 1.30 (s, 6H, H_9). ^{13}C NMR (mixture of rotamers) ($CDCl_3$, 101 MHz) δ (ppm): 163.5, 163.1, 151.0, 150.1, 149.9, 145.8, 145.1, 144.6, 143.9, 142.7, 141.4, 128.1, 123.9, 122.9, 120.5, 119.8, 119.7, 116.0, 111.8, 110.6, 108.3, 47.5, 46.9, 46.5, 40.3, 39.7, 36.1, 35.9, 32.5, 32.5, 32.0, 31.0, 30.8, 29.8, 28.9, 28.8, 19.2, 18.9. HRMS (ESI): *m/z* calcd. for $C_{27}H_{30}N_3O$ $[M+H]^+$ 412.2383; found 412.2381
Rf (10% MeOH in CH_2Cl_2): 0.73

7.4. SYNTHESIS OF COUMARIN 20

Methyl trifluoromethanesulfonate (61 μL, 0,54 mmol) was added to a solution of compound **20** (14.8 mg, 0.04 mmol) in CH_2Cl_2 (20 mL). The mixture was stirred overnight at room temperature under an Ar atmosphere and protected from light. Then, the solvent was removed under reduced pressure and the crude product was purified by column chromatography (silica gel, 0-4% MeOH in CH_2Cl_2) to give 11.6 mg (56 % yield) of a dark purple solid.

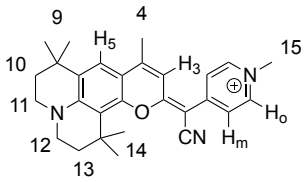

20

Dark purple solid.
^{1}H NMR ($CDCl_3$, 400 MHz): δ (ppm): 8.26 (d, J = 7.5 Hz, 2H, H_o), 7.89 (d, J = 7.5 Hz, 2H, H_m), 7.38 (s, 1H, H_5), 7.19 (s, 1H, H_3), 4.17 (s, 3H, H_{15}), 3.49 – 3.42 (m, 2H, H_{12}), 3.38 – 3.30 (m, 2H, H_{11}), 2.59 (s, 3H, H_4), 1.91 – 1.83 (m, 2H, H_{13}), 1.83 – 1.75 (m, 2H, H_{10}), 1.64 (s, 6H, H_{14}), 1.34 (s, 6H, H_9).
^{13}C NMR ($CDCl_3$, 101 MHz) δ (ppm): 167.0, 154.6, 152.6, 151.9, 148.1, 142.5, 131.8, 121.0, 120.3, 119.4, 114.9, 112.7, 109.1, 47.8, 47.0, 46.4, 39.4, 35.0, 32.7, 32.2, 30.1, 28.6, 19.6. HRMS (ESI): m/z calcd. for $C_{28}H_{32}N_3O^+$ $[M]^+$ 426.2540; found 426.2546
Rf (10% MeOH in CH_2Cl_2): 0.37

7.5. SYNTHESIS OF COUMARIN 21

Methyl 4-bromobutyrate (5.1 mL, 39.59 mmol) was added to a solution of **20** (1g, 2.42 mmol) in anhydrous ACN (300 mL). The mixture was stirred at 60ºC under an Ar atmosphere for 3 days. After removal of the solvent under vacuum, the product was purified by column chromatography (silica gel, 0-6% MeOH in CH_2Cl_2) and 672 mg (47 % yield) of a dark purple solid were obtained.

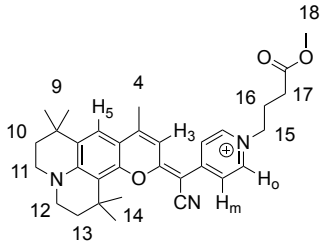

21

Dark purple solid.
^{1}H NMR ($CDCl_3$, 400 MHz): δ (ppm): δ 8.78 (d, *J* = 7.1 Hz, 2H, H_o), 7.93 (d, *J* = 7.2 Hz, 2H, H_m), 7.38 (s, 1H, H_5), 7.18 (s, 1H, H_3), 4.68 (t, *J* = 7.6 Hz, 2H, H_{15}), 3.69 (s, 3H, H_{18}), 3.48 – 3.40 (m, 2H, H_{12}), 3.38 – 3.29 (m, 2H, H_{11}), 2.62 (s, 3H, H_4), 2.56 (t, *J* = 6.7 Hz, 2H, H_{17}), 2.37 – 2.25 (m, 2H, H_{16}), 1.90 – 1.83 (m, 2H, H_{13}), 1.82 – 1.74 (m, 2H, H_{10}), 1.65 (s, 6H, H_{14}), 1.34 (s, 6H, H_9). ^{13}C NMR ($CDCl_3$, 101 MHz) δ (ppm): 173.1, 166.9, 154.1, 152.5, 151.7, 148.1, 142.3, 131.7, 121.1, 120.3, 119.3, 115.0, 112.6, 108.9, 58.1, 53.6, 52.1, 47.8, 47.0, 39.4, 35.0, 32.7, 32.3, 30.1, 28.6, 26.8, 19.8. HRMS (ESI): m/z calcd. for $C_{32}H_{38}N_3O_3^+$ $[M]^+$ 512.2908; found 512.2917
Rf (10% MeOH in CH_2Cl_2): 0.43

7.6. SYNTHESIS OF COUMARIN 22

A 1:2 (v/v) mixture of HCl (37%) and Mili-Q water (50 mL) was added to coumarin **21** (84 mg, 0.16 mmol). The reaction mixture was stirred at 60ºC for 3.5 hours protected from light. After removal of the solvent the crude product was used without further purification in the next reaction.

7.7. SYNTHESIS OF COUMARIN 23

Firstly, HATU (76.3 mg, 0.2 mmol), the linker N-Boc-1,3-diaminepropane hydrochloride (61.5 mg, 0.27 mmol) and the crude coumarin **22**, from previous reaction (section 7.6), were dried separately in a desiccator overnight. Secondly, HATU and the crude coumarin were dissolved in dry DMF (5mL and 4mL respectively), and the solution of HATU was added to that of the coumarin with 2 equivalents of DIPEA (69 μL, 0,2 mmol), and the resulting mixture was stirred for 10 minutes in the dark and under an Ar atmosphere. Then, the linker was dissolved in DMF (5 mL) and after addition of 1 equivalent of DIPEA, the solution was added to the previous mixture. The resulting mixture was stirred for 2 hours at room temperature, in the dark and under an Ar atmosphere. Finally, the solvent was removed under reduced pressure and the crude product was purified by column chromatography (0-15% MeOH in CH_2Cl_2) to give 43.2 mg (69 % yield) of a dark purple solid.

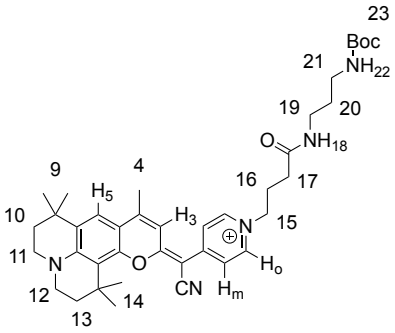

23

Dark purple solid.

^{1}H NMR ($CDCl_3$, 400 MHz): δ (ppm): 8.55 (d, J = 6.7 Hz, 2H, H_o), 8.48 (br s, 1H, H_{18}), 7.86 (d, J = 6.6 Hz, 2H, H_m), 7.37 (s, 1H, H_5), 7.29 (s, 1H, H_3), 5.40 (br s, 1H, H_{22}), 4.48 (t, J = 6.7 Hz, 2H, H_{15}), 3.47 – 3.39 (m, 2H, H_{12}), 3.39 – 3.31 (m, 2H, H_{11}), 3.30 – 3.23 (m, 2H, H_{19}), 3.21 – 3.09 (m, 2H, H_{21}), 2.61 (s, 3H, H_4), 2.54 (t, J = 6.6 Hz, 2H, H_{17}), 2.36 (qt, J = 6.7 Hz, 2H, H_{16}), 1.88 – 1.75 (m, 4H, H_{10}, H_{13}), 1.70 (qt, J = 6.3 Hz, 2H, H_{20}), 1.64 (s, 6H, H_{14}), 1.40 (s, 9H, H_{23}), 1.34 (s, 6H, H_9). LRMS (ESI): m/z calcd. for $C_{39}H_{52}N_5O_4^+$ $[M]^+$ 654.40; found 654.11

Rf (10% MeOH in CH_2Cl_2): 0.48

8. REFERENCES

1. Lavis, L. D.; Raines, R. T. Bright Ideas for Chemical Biology. *ACS Chem. Biol*. **2008**, *3*, 142-155.
2. Zheng, Q.; Juette, M.; Jockusch, S.; Wasserman, M.; Zhou, Z.; Altman, R.; Blanchard, S. Ultra-stable Organic Fluorophores for Single-molecule Research. *Chem. Soc. Rev*. **2014**, *43*, 1044-1056.
3. Lavis, L. D.; Raines, R. T. Bright Building Blocks for Chemical Biology. *ACS Chem. Biol*. **2014**, *9*, 855-866.
4. Owens, E.A.; Henary, M.; El Fakhri, G.; Choi, H. S. Tissue-Specific Near-Infrared Fluorescence Imaging. *Acc. Chem. Res*. **2016**, *49*, 1731-1740.
5. Cheng, Y.; Li, G.; Liu, Y.; Shi, Y.; Gao, G.; Wu, D.; Lan, J.; You, J. Unparalleled Ease of Access to a Library of Biheteroaryl Fluorophores via Oxidative Cross-Coupling Reactions: Discovery of Photostable NIR Probe for Mitochondria. *J. Am. Chem. Soc.* **2016**, *138*, 4730-4738.
6. Medina, F.; Marrero, J.; Macías-Alonso, M.; González, M.; Córdova-Guerrero, I.; Teissier García, A.; Osegueda-Robles, S. Coumarin heterocyclic derivatives: chemical synthesis and biological activity. *Nat. Prod. Rep.* **2015**, *32*, 1472-1507.
7. Gandioso, A.; Palau, M.; Bresolí-Obach, R.; Galindo, A.; Rovira, A.; Bosch, M.; Nonell, S.; Marchán, V. High Photostability in Nonconventional Coumarins with Far-Red/NIR Emission through Azetidinyl Substitution. *J. Org. Chem.* **2018**, *83*, 11519-11531.
8. de Moliner, F.; Kielland, N.; Lavilla, R.; Vendrell, M. Modern Synthetic Avenues for the Preparation of Functional Fluorophores. *Angew. Chem. Int. Ed.* **2017**, *56*, 3758-3769.
9. Gandioso, A.; Bresolí-Obach, R.; Nin-Hill, A.; Bosch, M.; Palau, M.; Galindo, A.; Contreras, S.; Rovira, A.; Rovira, C.; Nonell, S.; Marchán, V. Redisigning the Coumarin Scaffold into Small Bright Fluorophores with Far-Red to Near-Infrared Emission and Large Stokes Shifts Useful for Cell Imaging. *J. Org. Chem.* **2018**, *83*, 1185-1195.
10. Fonseca, A. S. C.; Soares, A. M. S.; Goncalves, M. S. T.; Costa, S. P. G. Thionated Coumarins and Quinolones in the Light Triggered Release of a Model Amino Acid: Synthesis and Photolysis Studies. *Tetrahedron*, **2012**, *68*, 7892-7900.
11. Rovira, A.; Pujals, M.; Gandioso, A.; López-Corrales, M.; Bosch, M.; Marchán, V. Modulating Photostability and Mitochondria Selectivity in Far-Red/NIR Emitting Coumarin Fluorophores through Replacement of Pyridinium by Pyrimidinium. *J. Org. Chem.* **2020**, *85*, 6086-6097.
12. Fournier, L.; Aujard, I.; Le Saux, T.; Maurin, S.; Beaupierre, S.; Baudin, J.-B.; Jullien, L. Coumarinylmethyl Caging Groups with Redshifted Absorption. *Chem. Eur. J.* **2013**, *19*, 17494-17507.
13. Gandioso, A.; Contreras, S.; Melnyk, I.; Oliva, J.; Nonell, S.; Velasco, D.; García-Amorós, J.; Marchán, V. *J. Org. Chem.* **2017**, *82*, 5398-5408.
14. López-Corrales, M.; Rovira, A.; Gandioso, A.; Bosch, M.; Nonell, S.; Marchán, V. Transformation of COUPY Fluorophores into a Novel Class of Visible-Light-Cleavable Photolabile Protecting Groups. *Chem. Eur. J.* **2020**, *26*, 16222-16227.
15. Anna Rovira, Doctoral Thesis in course.

16. Ozturk, T.; Ertas, E.; Mert, O. Use of Lawesson's Reagent in Organic Synthesis. *Chem. Rev*. **2007**, *107*, 5210-5278.
17. Rovira, A.; Gandioso, A.; Goñalons, M.; Galindo, A.; Massaguer, A.; Bosch, M.; Marchán, V. Solid-Phase Approaches for Labeling Targeting Peptides with Far-Red Emitting Coumarin Fluorophores. *J. Org. Chem.* **2019**, *84*, 1808-1817.

9. ACRONYMS

ACN: acetonitrile

Ar: argon

Calcd.: calculated

DCM: dichloromethane

DIPEA: *N,N*-diisopropylethylamine

DMF: *N,N*-dimethylformamide

HRMS (ESI): high resolution electrospray ionization mass spectrometry

EWG: electron-withdrawing group

HPLC: high-performance liquid chromatography

NMR: nuclear magnetic resonance

PPG: photolabile protecting group

Rf: retention factor in TLC

Rt: retention time in HPLC

NIR: near-infrared

TLC: thin layer chromatography

UV: ultraviolet

Vis: visible

APPENDICES

APPENDIX 1: HPLC-MS CHROMATOGRAMS OF THE PURE COMPOUNDS

Thiocoumarin 24

R_t = 25.2 min (analytical gradient: 10-100% in 30 min; A: 0.1% formic acid in H_2O, B: 0.1% formic acid in ACN)

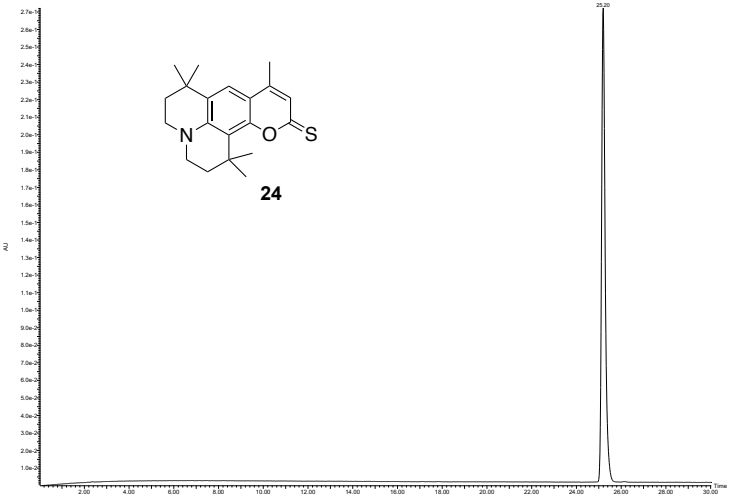

24

Coumarin scaffold 25

Rt = 17.2 min (analytical gradient: 10-100% in 30 min; A: 0.1% formic acid in H_2O, B: 0.1% formic acid in ACN).

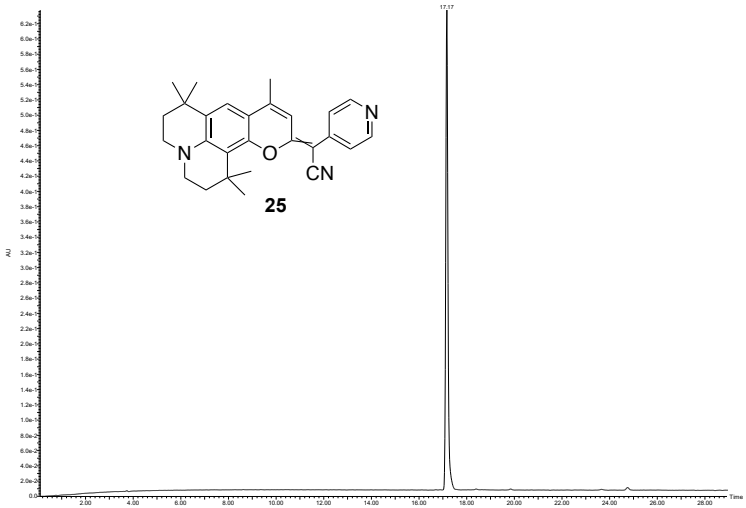

25

Coumarin 20

Rt = 16.2 min (analytical gradient: 10-100% in 30 min; A: 0.1% formic acid in H_2O, B: 0.1% formic acid in ACN).

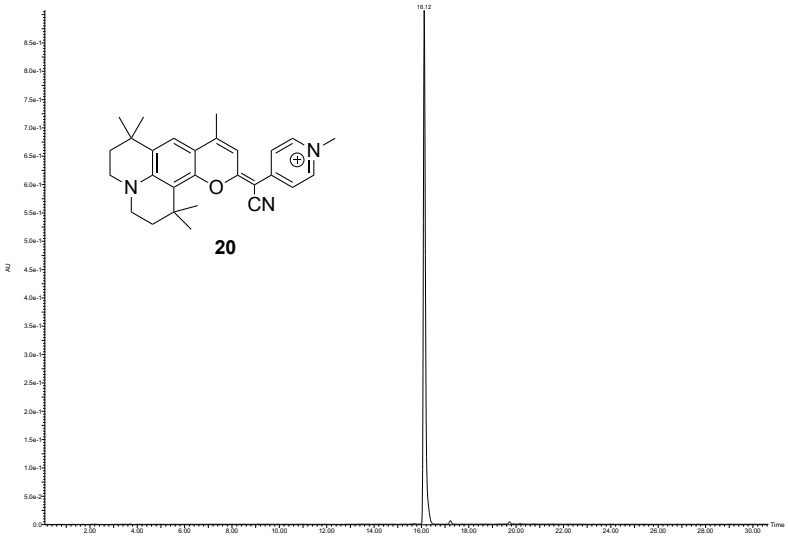

Coumarin 21

Rt = 7.3 min (analytical gradient: 30-100% in 15 min; A: 0.1% formic acid in H_2O, B: 0.1% formic acid in ACN).

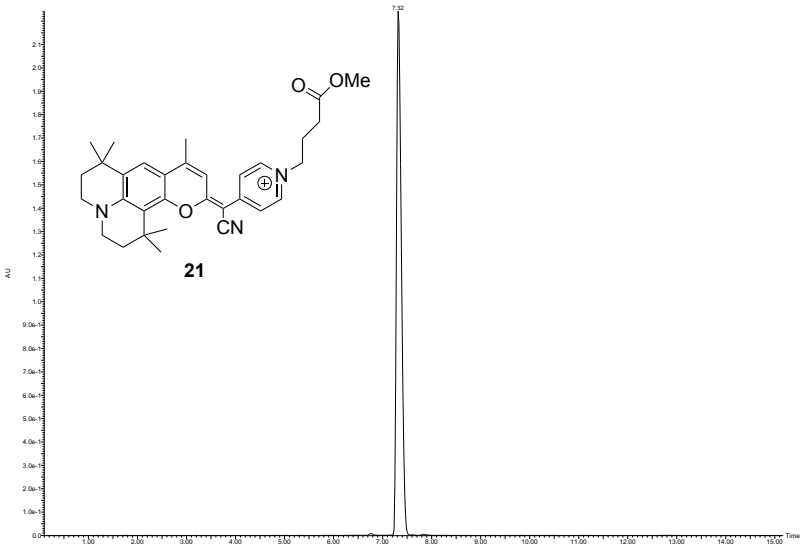

Coumarin 23

Rt = 9.7 min (analytical gradient: 10-100% in 15 min; A: 0.1% formic acid in H_2O, B: 0.1% formic acid in ACN).

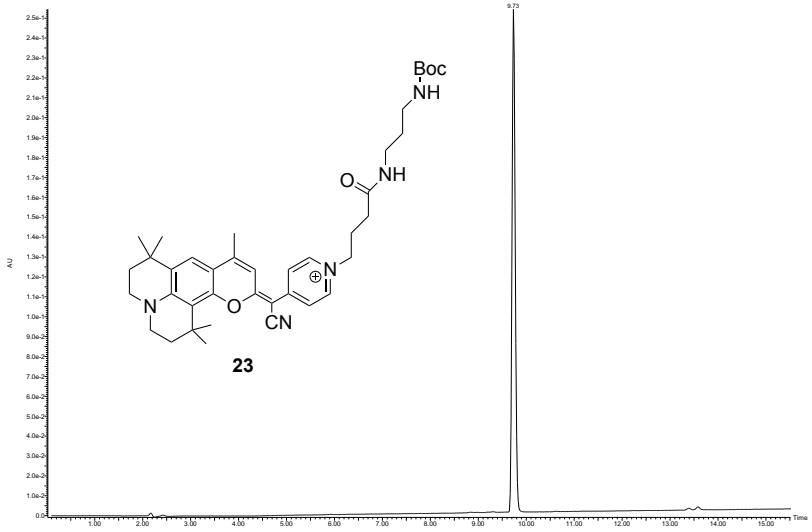

APPENDIX 2: ^{1}H AND ^{13}C NMR SPECTRA OF THE COMPOUNDS

Thiocoumarin 24

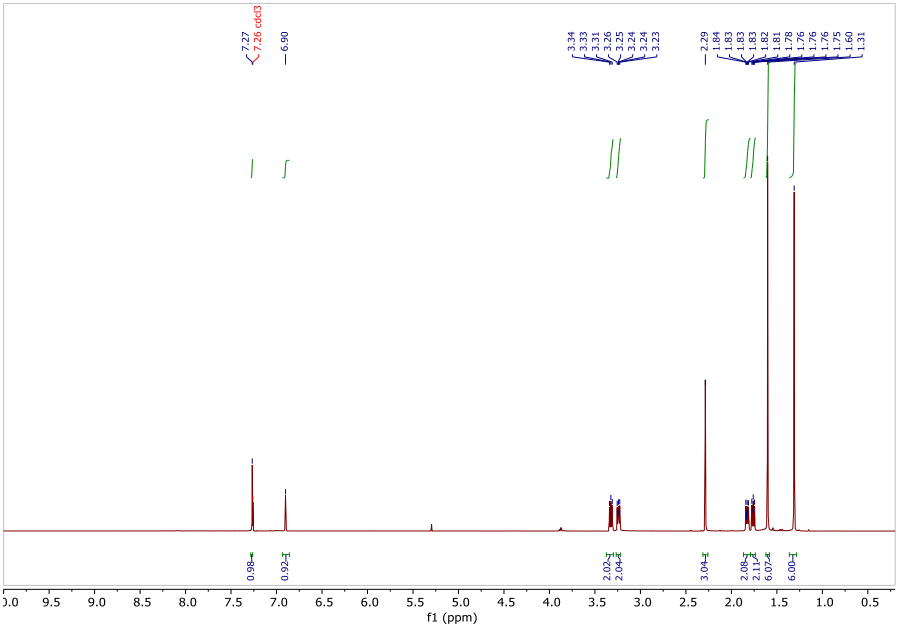

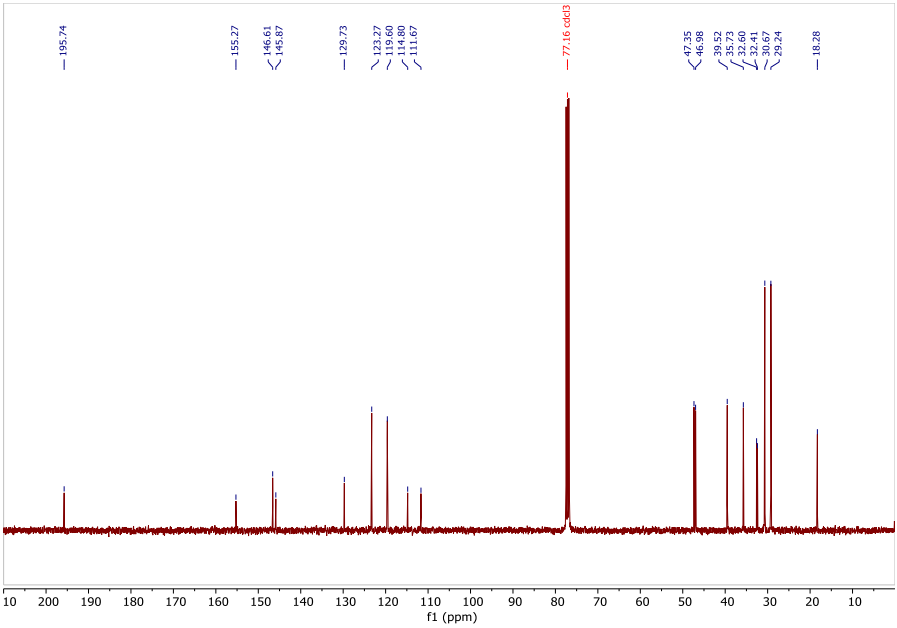

Coumarin scaffold 25

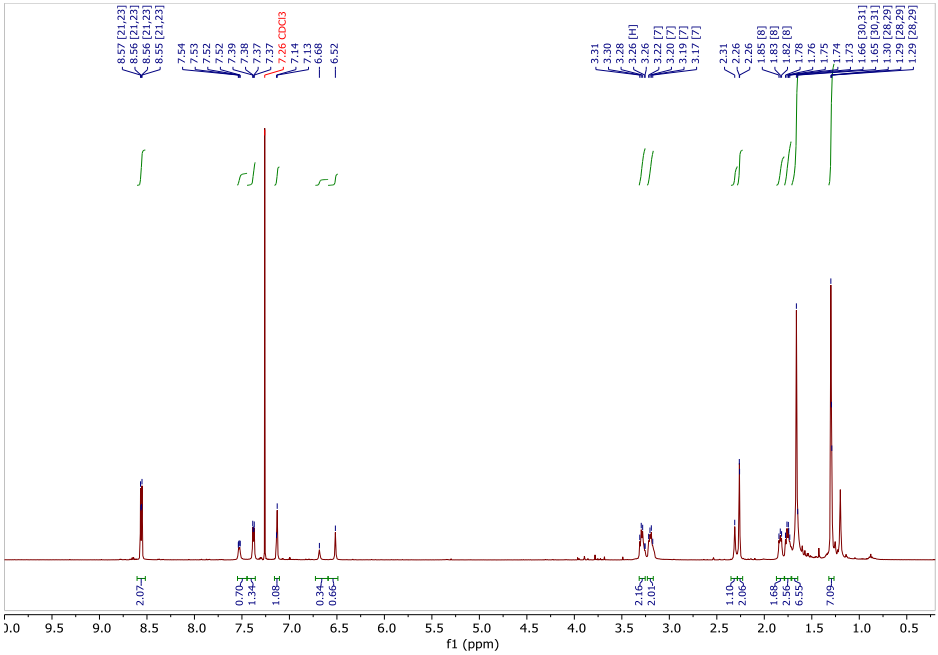

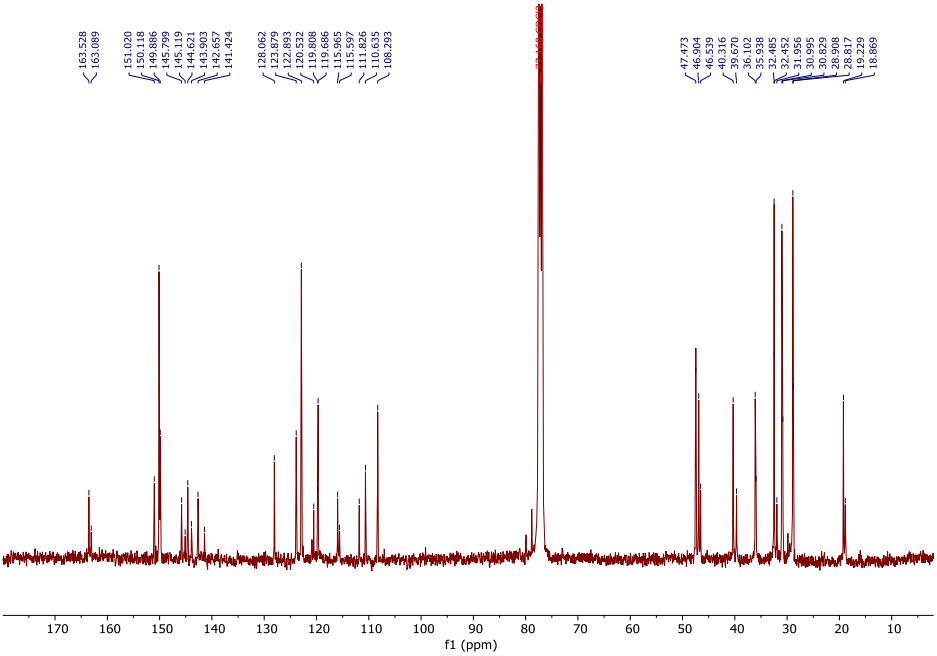

Coumarin 20

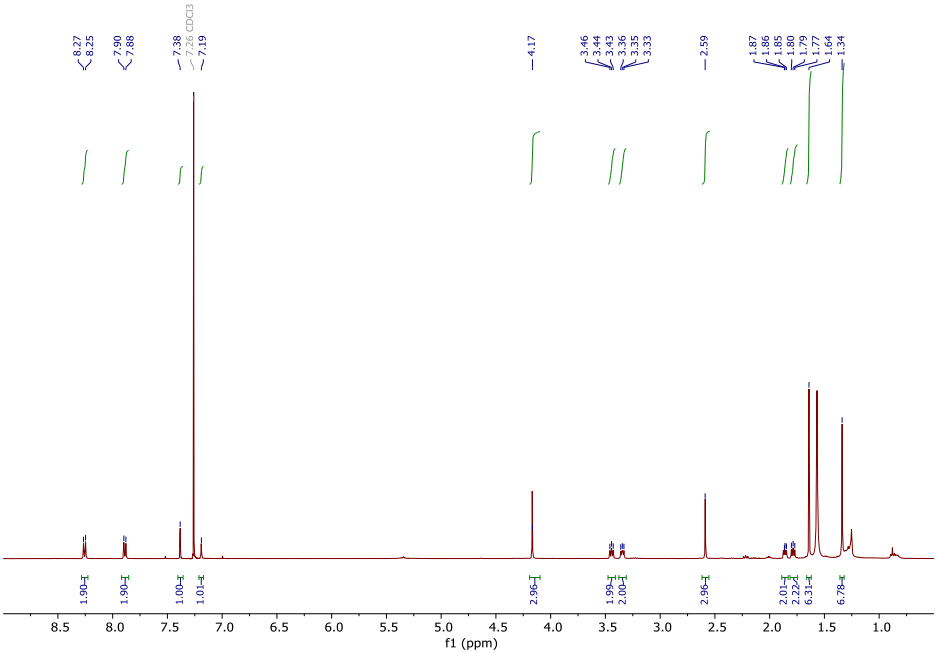
8.27
8.25
7.90
7.88
7.38
7.26 CDCl3
7.19
4.17
3.46
3.44
3.43
3.36
3.35
3.33
2.59
1.87
1.86
1.85
1.80
1.79
1.77
1.64
1.34
1.90
1.90
1.00
1.01
2.96
1.99
2.00
2.96
2.01
2.22
6.31
6.78
f1 (ppm)

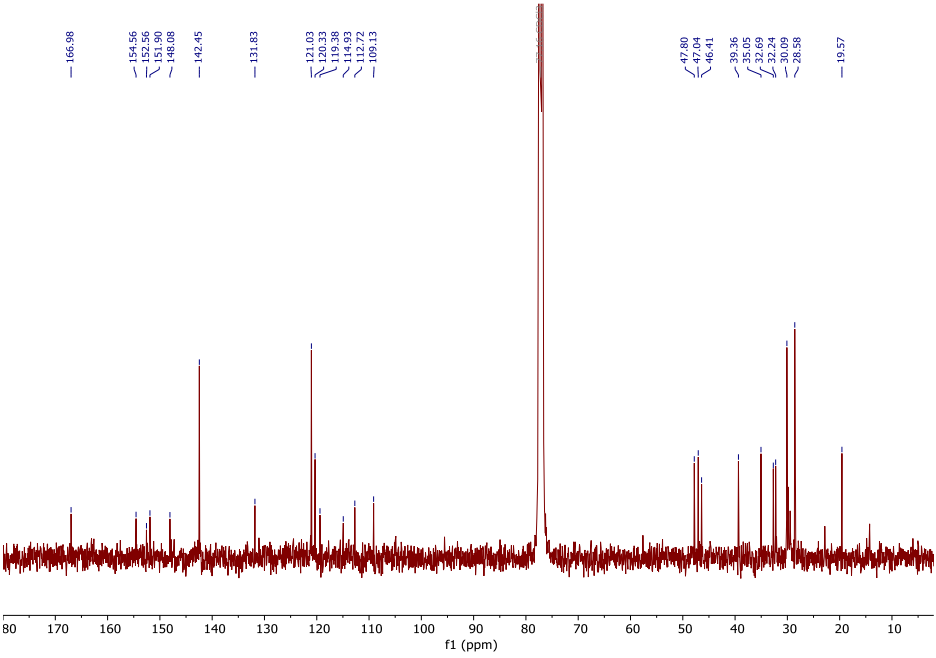
166.98
154.56
152.56
151.90
148.08
142.45
131.83
121.03
120.33
119.38
114.93
113.22
109.13
77.16
47.80
47.04
46.41
39.36
35.05
32.69
32.24
30.09
28.58
19.57
f1 (ppm)

Coumarin 21

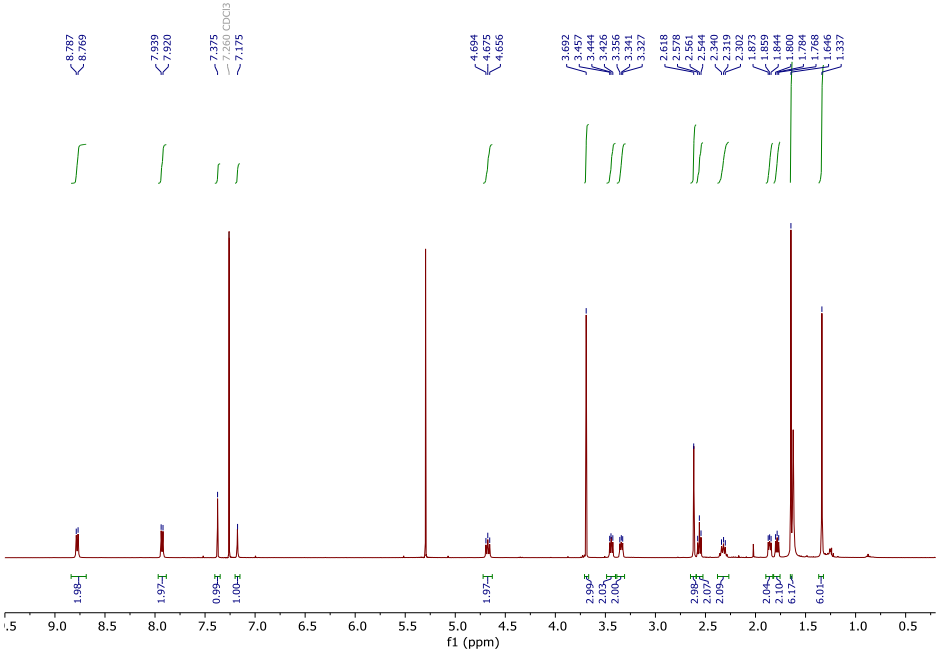
8.787
8.769
7.939
7.920
7.375
7.360
7.175
CDCl3
4.694
4.675
4.656
3.692
3.457
3.444
3.426
3.356
3.341
3.327
2.618
2.578
2.561
2.544
2.340
2.319
2.302
1.873
1.859
1.844
1.800
1.784
1.768
1.646
1.337
1.98
1.97
0.99
1.00
1.97
2.99
2.03
2.04
2.98
2.07
2.09
2.04
2.10
6.17
6.01
f1 (ppm)

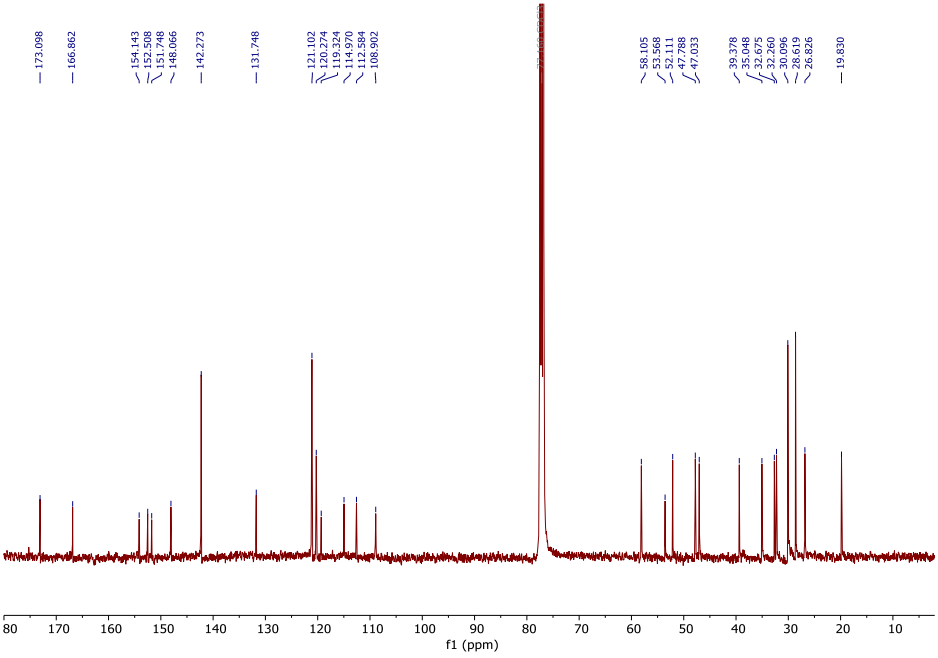
173.098
166.862
154.143
152.508
151.748
148.066
142.273
131.748
121.102
120.274
119.324
114.970
112.584
108.902
58.105
53.568
52.111
47.788
47.033
39.378
35.648
33.675
32.260
30.096
28.619
26.826
19.830
f1 (ppm)

Coumarin 23

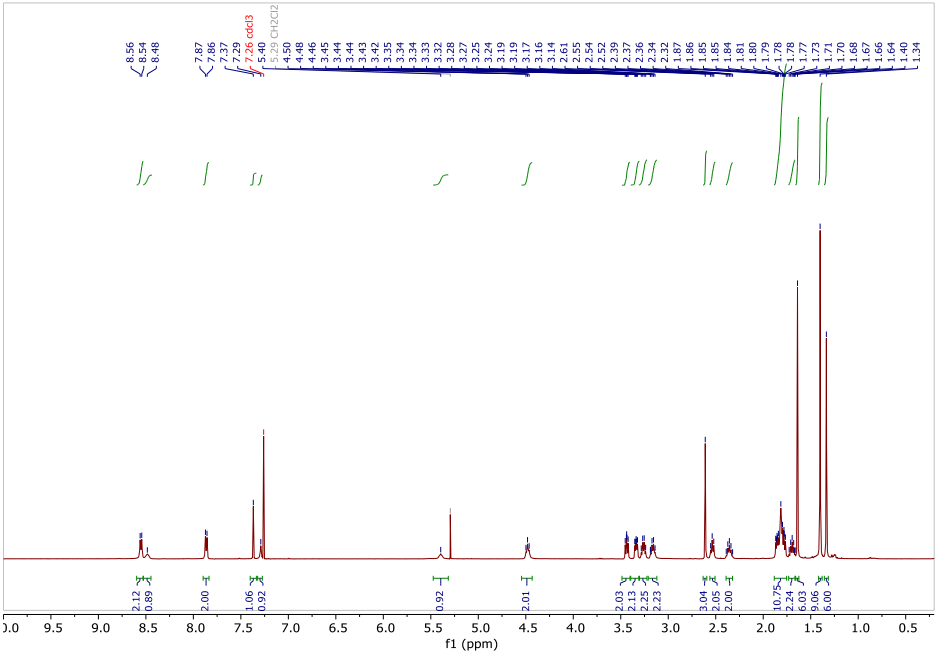
8.56
8.54
8.48
7.87
7.86
7.37
7.29
7.26 cdcl3
5.29 CH2Cl2
4.50
4.48
4.46
3.45
3.44
3.44
3.43
3.42
3.35
3.34
3.34
3.33
3.32
3.28
3.27
3.25
3.24
3.19
3.19
3.17
3.16
3.14
2.61
2.55
2.54
2.52
2.39
2.37
2.36
2.34
2.32
1.87
1.86
1.85
1.85
1.84
1.81
1.80
1.79
1.78
1.78
1.77
1.73
1.71
1.70
1.68
1.67
1.66
1.64
1.40
1.34
2.12
6.89
2.00
1.06
0.92
0.92
2.01
2.03
2.13
2.25
2.23
3.04
2.05
2.00
10.75
2.24
6.03
9.06
6.00
f1 (ppm)

APPENDIX 3: 2D NOESY NMR IN $CDCL_3$

Coumarin scaffold 25

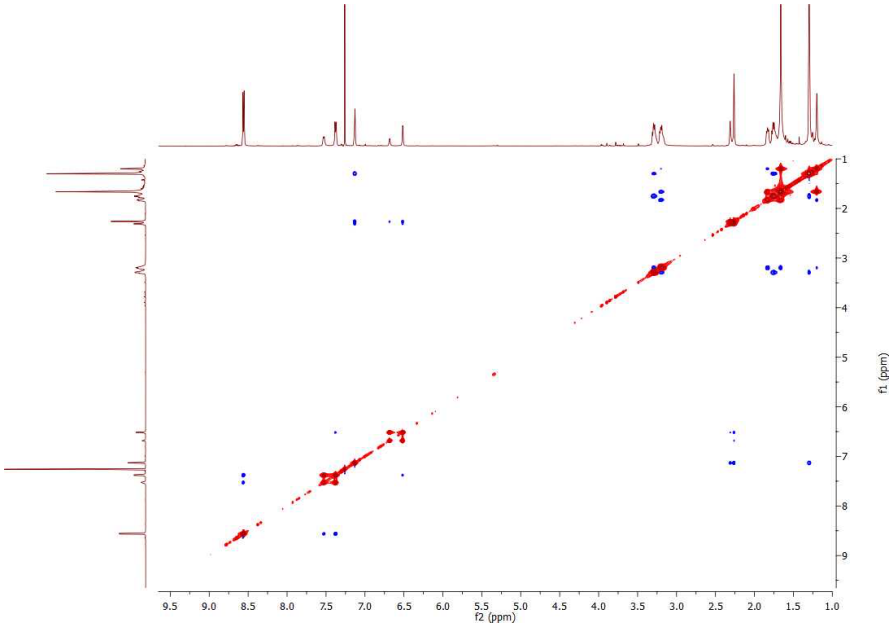

Coumarin 20

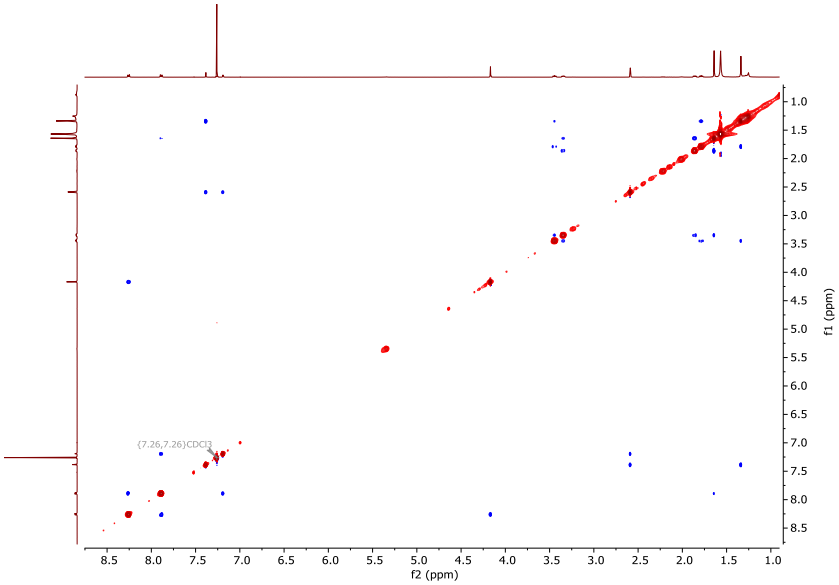

Coumarin 21